Graph-MVP: Multi-View Prototypical Contrastive Learning for Multiplex Graphs

Baoyu Jing[1], Yuejia Xiang[2], Xi Chen[2], Yu Chen[2], and Hanghang Tong[1]

[1] University of Illinois at Urbana-Champaign
[2] Platform and Content Group, Tencent
{baoyuj2, htong}@illinois.edu, {yuejiaxiang, jasonxchen, andyyuchen}@tencent.com

Abstract

Contrastive Learning (CL) is one of the most popular self-supervised learning frameworks for graph representation learning, which trains a Graph Neural Network (GNN) by discriminating positive and negative node pairs. However, there are two challenges for CL on graphs. On the one hand, traditional CL methods will unavoidably introduce semantic errors since they will treat some semantically similar nodes as negative pairs. On the other hand, most of the existing CL methods ignore the multiplexity nature of the real-world graphs, where nodes are connected by various relations and each relation represents a view of the graph. To address these challenges, we propose a novel Graph Multi-View Prototypical (Graph-MVP) framework to extract node embeddings on multiplex graphs. Firstly, we introduce a Graph Prototypical Contrastive Learning (Graph-PCL) framework to capture both node-level and semantic-level information for each view of multiplex graphs. Graph-PCL captures the node-level information by a simple yet effective data transformation technique. It captures the semantic-level information by an Expectation-Maximization (EM) algorithm, which alternatively performs clustering over node embeddings and parameter updating for GNN. Next, we introduce Graph-MVP based on Graph-PCL to jointly model different views of the multiplex graphs. Our key insight behind Graph-MVP is that different view-specific embeddings of the same node should have similar underlying semantic, based on which we propose two versions of Graph-MVP: Graph-MVP$_{hard}$ and Graph-MVP$_{soft}$ to align embeddings across views. Finally, we evaluate the proposed Graph-PCL and Graph-MVP on a variety of real-world datasets and downstream tasks. The experimental results demonstrate the effectiveness of the proposed Graph-PCL and Graph-MVP frameworks.

Introduction

The graph is a powerful representation of formalism and has been widely used to model relations among various objects, such as the citation relation and the same-author relation among papers. One of the primary challenges for graph representation learning is how to effectively encode nodes into informative embeddings such that they can be easily used in downstream tasks for extracting useful knowledge (Hamilton, Ying, and Leskovec 2017).

One of the predominant strategies in recent years is Contrastive Learning (CL), which aims to learn an effective Graph Neural Network (GNN) encoder such that similar nodes will be pulled together and dissimilar nodes will be pushed apart in the embedding space (Wu et al. 2021). The contrastive loss is usually designed to maximize the probabilities of the positive node pairs. Early methods, such as DeepWalk (Perozzi, Al-Rfou, and Skiena 2014) and node2vec (Grover and Leskovec 2016) sample positive node pairs based on their local proximity in the graphs. Recent methods rely on graph transformation or augmentation (Wu et al. 2021) to generate positive pairs and negative pairs, such as attribute based augmentation (Veličković et al. 2018; Hu et al. 2019; Jing, Park, and Tong 2021), structure based augmentation (Hassani and Khasahmadi 2020; You et al. 2020) sampling based augmentation (Qiu et al. 2020; Jiao et al. 2020) and adaptive augmentation (Zhu et al. 2021).

Despite the success of these methods, they only capture the node-level information but ignore the semantic-level information. This issue arises from the fact that node pairs are sampled regardless of their semantic similarity but just the topological proximity. For example, in an academic graph, two papers studying different sub-areas in graph learning (e.g., dynamic graphs v.s. graph alignment) might not topologically close to each other since they do not have a direct citation relation or same-author relation. Although they belong to the same area, they could still be treated as a negative pair by the existing methods. However, such a practice will inevitably induce semantic errors to the node embeddings, which has a negative influence on downstream machine learning models' performance even for simple tasks such as classification and clustering, not to mention complex tasks such as anomaly detection and graph alignment. To address this problem, inspired by (Li et al. 2020), we introduce a Graph Prototypical Contrastive Learning (Graph-PCL) to simultaneously capture both node-level and semantic-level information. For the node-level information, we propose a simple yet effective graph transformation technique along with a contrastive loss. The semantic-level CL is formulated as an Expectation-Maximization (EM) algorithm (Dempster, Laird, and Rubin 1977). In the E-step, a clustering algorithm is applied over node embeddings to extract prototypes (or semantic clusters). In the M-step, the parameters of the encoder are updated by minimizing the proposed loss.

In addition, most of the aforementioned methods ignore the multiplexity (De Domenico et al. 2013) of the real-world graphs, where nodes are connected by multiple types of relations and each relation is a view of the multiplex graph. In an academic graph, papers can be connected because of the same authors or keywords. In an entertainment graph, movies are related to each other since they share the same directors or actors. In a product graph, items have relations such as also-bought and also-view. Although it is viable to independently model each view and then combine the node embeddings of different views, different views might convey different, potentially complementary information and jointly considering them will usually produce more informative embeddings (Jing, Park, and Tong 2021; Park et al. 2020). To capture information across views, we further propose a novel Multi-View Prototypical (Graph-MVP) framework for multiplex graphs based on the Graph-PCL framework. Our key insight for multi-view modeling is that for a given node, its embeddings from different views should be semantically similar to each other. Based on this insight, we propose two versions of Graph-MVP: the hard constraint version Graph-MVP$_{hard}$ and the soft constraint version Graph-MVP$_{soft}$. Given a node, Graph-MVP$_{hard}$ enforces its node embeddings from different views should be in exactly the same semantic cluster, whereas Graph-MVP$_{soft}$ only requires their distributions over the semantic clusters to be similar.

The main contributions are summarized as follows:

- We present Graph-PCL which captures both node level and semantic level information.

- We propose a novel Graph-MVP with two versions Graph-MVP$_{hard}$ and Graph-MVP$_{soft}$ to jointly model different views of multiplex graphs.

- We comprehensively evaluate the proposed methods on a variety of real-world datasets and downstream tasks to demonstrate their effectiveness.

Preliminary

Problem Statement. Given a multiplex graph $\mathcal{G}_{\mathcal{M}}$, the task is to learn an encoder $\mathcal{E}$ mapping the node attribute matrix $\mathbf{X} \in \mathbb{R}^{N \times d_x}$ into node embeddings $\mathbf{H} \in \mathbb{R}^{N \times d}$ without using external labels, where N is the number of nodes, d_x and d are the dimensions.

Multiplex Graph. A multiplex graph with V views and N nodes is denoted as $\mathcal{G}_{\mathcal{M}} = \{\mathcal{G}^v\}_{v=1}^V$, where $\mathcal{G}^v(\mathbf{A}^v, \mathbf{X})$ is the v-th view graph, $\mathbf{A}^v \in \mathbb{R}^{N \times N}$ and $\mathbf{X} \in \mathbb{R}^{N \times d_x}$ are the adjacency and attribute matrices, and d_x is the dimension.

Methodology

We first present a Graph Prototypical Contrastive Learning (Graph-PCL) framework for a single view $\mathcal{G}^v = (\mathbf{A}^v, \mathbf{X})$, which simultaneously capture the node level and the semantic level information. Then we introduce a novel Graph Multi-View Prototypical (Graph-MVP) framework to jointly model different views of the multiplex graph $\mathcal{G}_{\mathcal{M}}$.
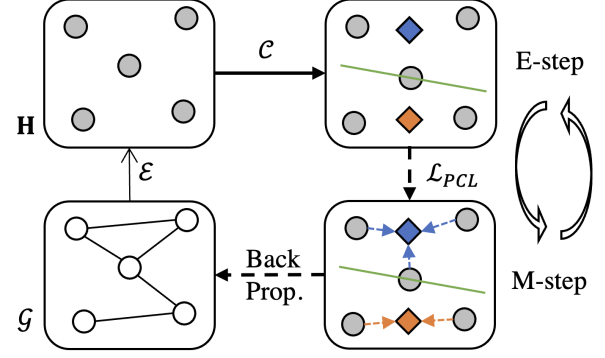

Figure 1: Illustration of Graph-PCL. $\mathcal{E}$ and $\mathcal{C}$ are the encoder and clustering algorithm. $\mathcal{G}$ is a view of $\mathcal{G}_{\mathcal{M}}$ and $\mathbf{H}$ is the embedding matrix. $\mathcal{L}_{PCL}$ is given in Equation (9). The circles and squares are nodes and cluster centers. The green line is the cluster boundary. "Back Prop." means back propagation.

Graph Prototypical Contrastive Learning

Node-level CL objects usually contain semantic errors since they will inevitably pair two semantically similar nodes as a negative training sample. To solve this issue, we introduce a Graph-PCL framework for a single view graph $\mathcal{G} = (\mathbf{A}, \mathbf{X})$[1] to capture both node-level and semantic-level information. An illustration of Graph-PCL is given in Figure 1. In the E-step, it applies a clustering algorithm $\mathcal{C}$ over embeddings $\mathbf{H}$. In the M-step, it updates $\mathcal{E}$ by minimizing $\mathcal{L}_{PCL}$.

Node-Level Loss. We present a simple yet effective graph transformation technique $\mathcal{T} = \{\mathcal{T}^+, \mathcal{T}^-\}$ along with a node-level contrastive loss.

Given an original graph $\mathcal{G} = (\mathbf{A}, \mathbf{X})$, the positive transformation $\mathcal{T}^+$ applies the dropout operation (Srivastava et al. 2014) over $\mathbf{A}$ and $\mathbf{X}$ with a pre-defined probability p_{drop}. We choose the dropout rather than the popular masking operation since the dropout will re-scale the outputs by $\frac{1}{1-p_{drop}}$ during training, which improves the training results. The negative transformation $\mathcal{T}^-$ is the random shuffle of $\mathbf{X}$. The transformed graphs are denoted by $\mathcal{G}^+ = \mathcal{T}^+(\mathcal{G})$ and $\mathcal{G}^- = \mathcal{T}^-(\mathcal{G})$, and the node embedding matrix of $\mathcal{G}$, $\mathcal{G}^+$ and $\mathcal{G}^-$ are thus $\mathbf{H} = \mathcal{E}(\mathcal{G})$, $\mathbf{H}^+ = \mathcal{E}(\mathcal{G}^+)$ and $\mathbf{H}^- = \mathcal{E}(\mathcal{G}^-)$.

We define the node-level contrastive loss as:

$$\mathcal{L}_{\mathcal{N}} = -\frac{1}{N} \sum_{n=1}^N \log \frac{\mathbf{e}^{cos(\mathbf{h}_n, \mathbf{h}_n^+)}}{\mathbf{e}^{cos(\mathbf{h}_n, \mathbf{h}_n^+)} + \mathbf{e}^{cos(\mathbf{h}_n, \mathbf{h}_n^-)}} \quad (1)$$

where $cos(,)$ denotes the cosine similarity, $\mathbf{h}_n$, $\mathbf{h}_n^+$ and $\mathbf{h}_n^-$ are the n-th rows of $\mathbf{H}$, $\mathbf{H}^+$ and $\mathbf{H}^-$.

Semantic Level Loss. Node-level contrastive loss is usually noisy, which will introduce semantic errors by treating two semantic similar nodes as a negative pair. To tackle this issue, we use a clustering algorithm $\mathcal{C}$ (e.g., K-means) to obtain the semantic clusters of nodes, and we use the EM algorithm to update the parameters of $\mathcal{E}$ to pull node embeddings closer to their assigned clusters (or prototypes).

---

[1]For clarity, we drop the script v when there's no ambiguity.

Our goal is to maximize the following log likelihood[2]:

$$\sum_{n=1}^{N} \log p(\mathbf{x}_n | \mathbf{\Theta}, \mathbf{C}) = \sum_{n=1}^{N} \log \sum_{k=1}^{K} p(\mathbf{x}_n, k | \mathbf{\Theta}, \mathbf{C}) \quad (2)$$

where $\mathbf{x}_n$ is the n-th row of $\mathbf{X}$, $\mathbf{\Theta}$ and $\mathbf{C}$ are the parameters of $\mathcal{E}$ and K-means algorithm $\mathcal{C}$, $k \in [1, \cdots, K]$ is the cluster label, and K is the number of clusters. Directly optimizing this objective is impracticable since the cluster label is a latent variable.

According to(Dempster, Laird, and Rubin 1977), the Evidence Lower Bound (ELBO) of Equation (2) is given by:

$$\text{ELBO} = \sum_{n=1}^{N} \sum_{k=1}^{K} Q(k|\mathbf{x}_n) \log \frac{p(\mathbf{x}_n, k | \mathbf{\Theta}, \mathbf{C})}{Q(k|\mathbf{x}_n)} \quad (3)$$

where $Q(k|\mathbf{x}_n) = p(k|\mathbf{x}_n, \mathbf{\Theta}, \mathbf{C})$ is the auxiliary function.

In the E-step, we fix $\mathbf{\Theta}$ so that we can estimate the cluster centers $\hat{\mathbf{C}}$ and the cluster assignments $\hat{Q}(k|\mathbf{x}_n)$ by running the K-means algorithm over the embeddings of the original graph $\mathbf{H} = \mathcal{E}(\mathcal{G})$. If a node $\mathbf{x}_n$ belongs to the cluster k, then its auxiliary function is an indicator function which satisfies $\hat{Q}(k|\mathbf{x}_n) = 1$, and $\hat{Q}(k'|\mathbf{x}_n) = 0$ for $\forall k' \neq k$.

In the M-step, based on $\hat{\mathbf{C}}$ and $\hat{Q}(k|\mathbf{x}_n)$ obtained in the E-step, we update $\mathbf{\Theta}$ by maximizing ELBO:

$$\begin{aligned}
\text{ELBO} = &\sum_{n=1}^{N} \sum_{k=1}^{K} \hat{Q}(k|\mathbf{x}_n) \log p(\mathbf{x}_n, k | \mathbf{\Theta}, \hat{\mathbf{C}}) \\
&- \sum_{n=1}^{N} \sum_{k=1}^{K} \hat{Q}(k|\mathbf{x}_n) \log \hat{Q}(k|\mathbf{x}_n)
\end{aligned} \quad (4)$$

Dropping the second term of the above equation, which is a constant, we will minimize the following loss function:

$$\mathcal{L}_{\mathcal{S}} = -\sum_{n=1}^{N} \sum_{k=1}^{K} \hat{Q}(k|\mathbf{x}_n) \log p(\mathbf{x}_n, k | \mathbf{\Theta}, \hat{\mathbf{C}}) \quad (5)$$

Assuming a uniform prior distribution over $\mathbf{x}_n$, we have:

$$p(\mathbf{x}_n, k | \mathbf{\Theta}, \hat{\mathbf{C}}) \propto p(k|\mathbf{x}_n, \mathbf{\Theta}, \hat{\mathbf{C}}) \quad (6)$$

We define $p(k|\mathbf{x}_n, \mathbf{\Theta}, \hat{\mathbf{C}})$ by:

$$p(k|\mathbf{x}_n, \mathbf{\Theta}, \hat{\mathbf{C}}) = \frac{\mathbf{e}^{(\hat{\mathbf{c}}_k^T \cdot \mathbf{h}_n / \tau)}}{\sum_{k'=1}^{K} \mathbf{e}^{(\hat{\mathbf{c}}_{k'}^T \cdot \mathbf{h}_n / \tau)}} \quad (7)$$

where $\mathbf{h}_n \in \mathbb{R}^d$ is the embedding of $\mathbf{x}_n$, $\hat{\mathbf{c}}_k \in \mathbb{R}^d$ is the vector of the k-th cluster center, τ is the temperature.

Let's use l_n to denote the cluster label of $\mathbf{x}_n$, and normalize the loss by $\frac{1}{N}$, then Equation (5) can be rewritten as:

$$\mathcal{L}_{\mathcal{S}} = -\frac{1}{N} \sum_{n=1}^{N} \log \frac{\mathbf{e}^{(\hat{\mathbf{c}}_{l_n}^T \cdot \mathbf{h}_n / \tau)}}{\sum_{k=1}^{K} \mathbf{e}^{(\hat{\mathbf{c}}_k^T \cdot \mathbf{h}_n / \tau)}} \quad (8)$$

Overall Loss. Combing the node-level loss in Equation (1) and the semantic-level loss in Equation (8), we have:

$$\mathcal{L}_{PCL} = \lambda_{\mathcal{N}} \mathcal{L}_{\mathcal{N}} + \lambda_{\mathcal{S}} \mathcal{L}_{\mathcal{S}} \quad (9)$$

where $\lambda_{\mathcal{N}}$ and $\lambda_{\mathcal{S}}$ are tunable hyper-parameters.

---

[2]In $p(\mathbf{x}_n | \mathbf{\Theta}, \mathbf{C})$, the condition $\mathbf{A}$ is omitted for clarity.

Graph Multi-View Prototypical Framework

The real-world graphs are multiplex in nature, where nodes are connected by multiple relations and each relation is a view of the multiplex graph. We propose a novel Graph-MVP to jointly capture both the node-level and semantic-level information across views. We first introduce the node-level loss function for multiplex graphs. Then we introduce the semantic-level loss function, with the insight that for the same node $\mathbf{x}_n$, the *semantic codes* $\{\mathbf{p}_n^v\}_{v=1}^V$ of its view-specific embeddings $\{\mathbf{h}_n^v\}_{v=1}^V$ should be similar to each other. Two versions: Graph-MVP$_{hard}$ and Graph-MVP$_{soft}$ are proposed to semantically align $\{\mathbf{h}_n^v\}_{v=1}^V$ with hard and soft constraints, respectively.

Node Level Loss. Given $\mathcal{G}_{\mathcal{M}} = \{\mathcal{G}^v\}_{v=1}^V$, we use $\{\mathcal{E}^v\}_{v=1}^V$ to extract view-specific embeddings $\{\mathbf{H}^v\}_{v=1}^V$. We use the same graph transformation technique $\mathcal{T} = \{\mathcal{T}^+, \mathcal{T}^-\}$ as in Graph-PCL to obtain the positive and negative node embeddings $\{\mathbf{H}^{v+}\}_{v=1}^V$ and $\{\mathbf{H}^{v-}\}_{v=1}^V$.

For a node $\mathbf{x}_n$, we define its *global embedding vector* as the concatenation of its view-specific embeddings $\mathbf{h}_n = [\mathbf{h}_n^1, \cdots, \mathbf{h}_n^V] \in \mathbb{R}^{V \times d}$. Its positive and negative global embeddings are defined as $\mathbf{h}_n^+ = [\mathbf{h}_n^{1+}, \cdots, \mathbf{h}_n^{V+}] \in \mathbb{R}^{V \times d}$ and $\mathbf{h}_n^- = [\mathbf{h}_n^{1-}, \cdots, \mathbf{h}_n^{V-}] \in \mathbb{R}^{V \times d}$.

The node-level loss of Graph-MVP is comprised of both local and global contrastive loss, which is given by

$$\mathcal{L}_{\mathcal{N}} = \sum_{v=1}^{V} \lambda_{\mathcal{N}}^v \mathcal{L}_{\mathcal{N}}^v + \lambda_{\mathcal{N}}^{global} \mathcal{L}_{\mathcal{N}}^{global} \quad (10)$$

where $\mathcal{L}_{\mathcal{N}}^v$ is the loss for view v, $\mathcal{L}_{\mathcal{N}}^{global}$ is the loss for the global embedding vector pairs, $\lambda_{\mathcal{N}}^v$ and $\lambda_{\mathcal{N}}^{global}$ are tunable hyper-parameters. The mathematical formulations for both of $\mathcal{L}_{\mathcal{N}}^v$ and $\mathcal{L}_{\mathcal{N}}^{global}$ are given in Equation (1).

Hard Constraint. To enforce $\{\mathbf{h}_n^v\}_{v=1}^V$ to have the same semantic code $\mathbf{p}_n^v = \mathbf{p}_n, \forall v \in [1, \cdots, V]$, we propose to directly apply K-means algorithm over the global embedding vector $\mathbf{h}_n = [\mathbf{h}_n^1, \cdots, \mathbf{h}_n^V]$, and then calculate $\mathbf{p}_n$ based on the global embedding vector $\mathbf{h}_n$ by Equation (7).

The hard constraint version Graph-MVP$_{hard}$ works similar as Graph-PCL: In the E-step, the K-means algorithm is applied on the global embedding vectors; In the M-step, we minimize the following loss:

$$\mathcal{L}_{MVP}^{hard} = \lambda_{\mathcal{N}} \mathcal{L}_{\mathcal{N}} + \lambda_{\mathcal{S}} \mathcal{L}_{\mathcal{S}} \quad (11)$$

where $\mathcal{L}_{\mathcal{N}}$ and $\mathcal{L}_{\mathcal{S}}$ are given in Equation (10) and (8).

Soft Constraint. Different from the hard constraint which enforces exactly the same semantic code for $\{\mathbf{h}_n^v\}_{v=1}^V$, the soft constraint only requires that given a set of cluster centers $\hat{\mathbf{C}}$, the semantic codes $\{\mathbf{p}_n^v\}_{v=1}^V$, i.e., semantic distributions, of $\{\mathbf{h}_n^v\}_{v=1}^V$ over these centers are similar. An illustration of the soft constraint is provided in Figure 2.

The soft constraint version Graph-MVP$_{soft}$ will first apply separate K-means algorithm $\{\mathcal{C}^v\}_{v=1}^V$ for each view, and then it will obtain the cluster centers of different views $\{\hat{\mathbf{C}}^v \in \mathbb{R}^{K^v \times d}\}_{v=1}^V$, where K^v is the number of clusters for view v.

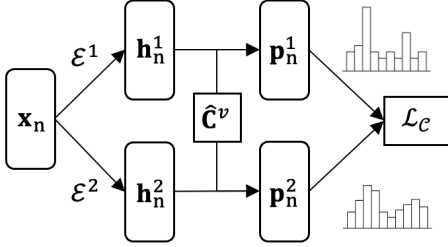| Graphs	# Nodes	Views	# Edges	# Attributes	# Labeled Data	# Classes
ACM	3,025	Paper-Subject-Paper (PSP)	2,210,761	1,830	600	3
		Paper-Author-Paper (PAP)	29,281	(Paper Abstract)		
IMDB	3,550	Movie-Actor-Movie (MAM)	66,428	1,007	300	3
		Movie-Director-Movie (MDM)	13,788	(Movie plot)		
DBLP	7,907	Paper-Author-Paper (PAP)	144,783	2,000	80	4
		Paper-Paper-Paper (PPP)	90,145	(Paper Abstract)		
		Paper-Author-Term-Author-Paper (PATAP)	57,137,515			
Amazon	7,621	Item-AlsoView-Item (IVI)	266,237	2,000	80	4
		Item-AlsoBought-Item (IBI)	1,104,257	(Item description)		
		Item-BoughtTogether-Item (IOI)	16,305			

Table 1: Statistics of the graphs

Figure 2: Illustration of the soft constraint. $\mathbf{x}_n$ is the node attribute vector. $\mathbf{h}_n^1$ and $\mathbf{h}_n^2$ are the view-specific embeddings of $\mathbf{x}_n$. $\hat{\mathbf{C}}^v$ is the cluster center matrix. $\mathbf{p}_n^1$ and $\mathbf{p}_n^2$ are the semantic codes, and $\mathcal{L}_{\mathcal{C}}$ is given in Equation (12).

Given a set of cluster centers $\hat{\mathbf{C}}^v$, we obtain the semantic codes $\{\mathbf{p}_n^i \in \mathbb{R}^{K^v}\}_{i=1}^V$ for $\{\mathbf{h}_n^i\}_{i=1}^V$ via Equation (7). Then we use Cross Entropy (CE) loss among $\{\mathbf{p}_n^i\}_{i=1}^V$ to enforce their distributional similarities:

$$\mathcal{L}_{\mathcal{C}}(\mathbf{x}_n, \hat{\mathbf{C}}^v) = \frac{1}{V^2 - V} \sum_{\substack{i,j=1 \\ i \neq j}}^V H(\mathbf{p}_n^i, \mathbf{p}_n^j) \qquad (12)$$

We use CE rather than KL-divergence, since CE encourages $\mathbf{p}$ to concentrate probabilities to a single cluster k, which has a better performance in experiments. Note that $H(\mathbf{p}, \mathbf{q}) = KL(\mathbf{p}, \mathbf{q}) + H(\mathbf{p})$, and the minimum $H(\mathbf{p})$ is achieved when $\mathbf{p}[k] = 1$ and $\mathbf{p}[k'] = 0$, $k' \neq k$.

Thus, we have the total loss for N nodes and V views:

$$\mathcal{L}_{\mathcal{C}} = \frac{1}{N} \sum_{n=1}^N \sum_{v=1}^V \mathcal{L}_{\mathcal{C}}(\mathbf{x}_n, \hat{\mathbf{C}}^v) \qquad (13)$$

Finally, we have the total loss for Graph-MVP$_{soft}$:

$$\mathcal{L}_{MVP}^{soft} = \lambda_{\mathcal{N}} \mathcal{L}_{\mathcal{N}} + \lambda_{\mathcal{S}} \mathcal{L}_{\mathcal{S}} + \lambda_{\mathcal{C}} \mathcal{L}_{\mathcal{C}} \qquad (14)$$

where $\mathcal{L}_{\mathcal{N}}$, $\mathcal{L}_{\mathcal{S}}$ and $\mathcal{L}_{\mathcal{C}}$ are given in Equation (10) (8) (13).

Experiments

Experimental Setups

Datasets. Following (Park, Han, and Yu 2020; Jing, Park, and Tong 2021), we evaluate our methods on four real-word multiplex graphs: ACM, IMDB, DBLP and Amazon. The statistics of these graphs are presented in Table 1. For more detailed descriptions, please refer to (Park et al. 2020).

Comparison Methods. We compare with representative methods for **(1) graphs**, including methods disregarding attributes: DeepWalk (Perozzi, Al-Rfou, and Skiena 2014) and node2vec (Grover and Leskovec 2016), and methods considering attributes: GCN (Kipf and Welling 2016), GAT (Veličković et al. 2017), DGI (Veličković et al. 2018), ANRL (Zhang et al. 2018b), CAN (Meng et al. 2019), DGCN (Zhuang and Ma 2018) and HDI (Jing, Park, and Tong 2021). **(2) multiplex graphs**, including methods disregarding attributes: CMNA (Chu et al. 2019), MNE (Zhang et al. 2018a), and methods considering attributes: mGCN (Ma et al. 2019), HAN (Wang et al. 2019b), DMGI, DMGI$_{attn}$ (Park et al. 2020) and HDMI (Jing, Park, and Tong 2021).

Evaluation Metrics. Following (Park et al. 2020), we first extract node embeddings from the trained encoder. Then we train downstream models with the extracted embeddings, and evaluate models' performance on the following tasks: **(1) a supervised task**: node classification; **(2) unsupervised tasks**: node clustering and similarity search. For the node classification task, we train a logistic regression model and evaluate its performance with Macro-F1 (MaF1) and Micro-F1 (MiF1). For the node clustering task, we train the K-means algorithm and evaluate it with Normalized Mutual Information (NMI). For the similarity search task, we first calculate the cosine similarity for each pair of nodes, and for each node, we compute the rate of the nodes to have the same label within its 5 most similar nodes (S@5).

Implementation Details. We use the one layer 1st-order GCN (Kipf and Welling 2016) as the encoder $\mathcal{E}^v = \text{Tanh}(\mathbf{X}\mathbf{A}^v\mathbf{W} + \mathbf{X}\mathbf{W}' + \mathbf{b})$. We set dimension $d = 128$ and $p_{drop} = 0.5$. During training, we first warm up the encoders by $\mathcal{L}_{\mathcal{N}}$ with the learning rate of 0.005. Then we apply the overall losses with the learning rate of 0.005 for IMDB and 0.001 for other graphs. We tune the parameters $\lambda_{\mathcal{N}}$, $\lambda_{\mathcal{S}}$ and $\lambda_{\mathcal{C}} \in \{1, 0.1, 0.01, 0.001, 0.0001\}$, and $\tau \in \{0.01, 0.02, 0.05, 0.1, 0.2, 0.5, 1, 2, 5, 10, 20, 50, 100\}$, and $K \in [3, 4, 5, 10, 20, 30, 50]$. We adopt early stopping with the patience of 100 to prevent overfitting. In the M-step, we train the models for 5 epochs. To obtain the final node embeddings of the multiplex graphs for both Graph-MVP and Graph-PCL, we either use average pooling or concatenation over the view-specific embeddings, and report the best results. The models are implemented by PyTorch (Paszke et al. 2019) and trained on NVIDIA RTX 3080.

Dataset	ACM				IMDB				DBLP				Amazon			
Metric	MaF1	MiF1	NMI	S@5	MaF1	MiF1	NMI	S@5	MaF1	MiF1	NMI	S@5	MaF1	MiF1	NMI	S@5
DeepWalk	0.739	0.748	0.310	0.710	0.532	0.550	0.117	0.490	0.533	0.537	0.348	0.629	0.663	0.671	0.083	0.726
node2vec	0.741	0.749	0.309	0.710	0.533	0.550	0.123	0.487	0.543	0.547	0.382	0.629	0.662	0.669	0.074	0.738
GCN/GAT	0.869	0.870	0.671	0.867	0.603	0.611	0.176	0.565	0.734	0.717	0.465	0.724	0.646	0.649	0.287	0.624
DGI	0.881	0.881	0.640	0.889	0.598	0.606	0.182	0.578	0.723	0.720	0.551	0.786	0.403	0.418	0.007	0.558
ANRL	0.819	0.820	0.515	0.814	0.573	0.576	0.163	0.527	0.770	0.699	0.332	0.720	0.692	0.690	0.166	0.763
CAN	0.590	0.636	0.504	0.836	0.577	0.588	0.074	0.544	0.702	0.694	0.323	0.792	0.498	0.499	0.001	0.537
DGCN	0.888	0.888	0.691	0.690	0.582	0.592	0.143	0.179	0.707	0.698	0.462	0.491	0.478	0.509	0.143	0.194
HDI	0.901	0.900	0.650	0.900	0.634	0.638	0.194	0.605	0.814	0.800	0.570	0.799	0.804	0.806	0.487	0.856
CMNA	0.782	0.788	0.498	0.363	0.549	0.566	0.152	0.069	0.566	0.561	0.420	0.511	0.657	0.665	0.070	0.435
MNE	0.792	0.797	0.545	0.791	0.552	0.574	0.013	0.482	0.566	0.562	0.136	0.711	0.556	0.567	0.001	0.395
mGCN	0.858	0.860	0.668	0.873	0.623	0.630	0.183	0.550	0.725	0.713	0.468	0.726	0.660	0.661	0.301	0.630
HAN	0.878	0.879	0.658	0.872	0.599	0.607	0.164	0.561	0.716	0.708	0.472	0.779	0.501	0.509	0.029	0.495
DMGI	0.898	0.898	0.687	0.898	0.648	0.648	0.196	0.605	0.771	0.766	0.409	0.766	0.746	0.748	0.425	0.816
DMGI$_{attn}$	0.887	0.887	0.702	0.901	0.602	0.606	0.185	0.586	0.778	0.770	0.554	0.798	0.758	0.758	0.412	0.825
HDMI	0.901	0.901	0.695	0.898	0.650	0.658	0.198	0.607	0.820	**0.811**	0.582	**0.809**	0.808	0.812	0.500	0.857
Graph-PCL	0.901	0.901	0.737	0.914	0.653	0.656	**0.228**	0.612	0.790	0.774	0.553	0.799	0.830	0.829	0.540	**0.905**
Graph-MVP$_{hard}$	0.902	0.902	0.706	0.913	**0.658**	**0.664**	0.223	0.602	**0.822**	0.809	**0.607**	0.801	**0.854**	0.851	**0.564**	0.904
Graph-MVP$_{soft}$	**0.916**	**0.914**	**0.756**	**0.918**	**0.658**	0.659	0.219	**0.613**	0.802	0.796	0.593	0.785	**0.854**	**0.852**	**0.564**	0.903

Table 2: Overall Performance on Multiplex Graphs

Dataset	ACM				IMDB				DBLP						Amazon					
View	PSP		PAP		MDM		MAM		PAP		PPP		PATAP		IVI		IBI		IOI	
Metric	MaF1	MiF1	MaF1	MiF1	MaF1	MiF1	MaF1	MiF1	MaF1	MiF1	MaF1	MiF1	MaF1	MiF1	MaF1	MiF1	MaF1	MiF1	MaF1	MiF1
DGI	0.663	0.668	0.855	0.853	0.573	0.586	0.558	0.564	0.804	0.796	0.728	0.717	0.240	0.272	0.380	0.388	0.386	0.410	0.569	0.574
HDI	0.742	0.744	0.889	0.888	0.626	0.631	0.600	0.606	0.812	**0.803**	0.751	0.745	0.241	0.284	0.581	0.583	0.524	0.529	0.796	0.799
Graph-PCL	**0.833**	**0.836**	**0.908**	**0.908**	**0.649**	**0.653**	**0.653**	**0.652**	**0.816**	0.803	**0.768**	**0.763**	**0.760**	**0.750**	**0.849**	**0.848**	**0.850**	**0.848**	**0.851**	**0.851**

Metric	MaF1	MiF1	MaF1	MiF1	MaF1	MiF1	MaF1	FiF1	MaF1	MiF1
Graph-PCL	0.901	0.901	0.653	0.656	0.790	0.774			0.830	0.829
Graph-MVP$_{hard}$	0.902	0.902	**0.658**	**0.664**	**0.822**	**0.809**			**0.854**	0.851
Graph-MVP$_{soft}$	**0.916**	**0.914**	**0.658**	0.659	0.802	0.796			**0.854**	**0.852**

Table 3: Overall Performance on Each View: Node Classification. The lower part is copied from Table 2.

Dataset	ACM				IMDB				DBLP						Amazon					
View	PSP		PAP		MDM		MAM		PAP		PPP		PATAP		IVI		IBI		IOI	
Metric	NMI	S@5	NMI	S@5	NMI	S@5	NMI	S@5	NMI	S@5	NMI	S@5	NMI	S@5	NMI	S@5	NMI	S@5	NMI	S@5
DGI	0.526	0.698	0.651	0.872	0.145	0.549	0.089	0.495	0.547	0.800	0.404	0.741	0.054	0.583	0.002	0.395	0.003	0.414	0.038	0.701
HDI	0.528	0.716	0.662	0.886	0.194	0.592	0.143	0.527	0.562	0.805	0.408	0.742	0.054	0.591	0.169	0.544	0.153	0.525	0.407	0.826
Graph-PCL	**0.600**	**0.851**	**0.735**	**0.917**	**0.210**	**0.602**	**0.180**	**0.585**	**0.599**	**0.807**	**0.501**	**0.752**	**0.473**	**0.733**	**0.551**	**0.901**	**0.544**	**0.903**	**0.536**	**0.905**

Metric	NMI	S@5	NMI	S@5	NMI	S@5	NMI	S@5
Graph-PCL	0.737	0.914	**0.228**	0.612	0.553	0.799	0.540	**0.905**
Graph-MVP$_{hard}$	0.706	0.913	0.223	0.602	**0.607**	**0.801**	**0.564**	0.904
Graph-MVP$_{soft}$	**0.756**	**0.918**	0.219	**0.613**	0.593	0.785	**0.564**	0.903

Table 4: Overall Performance on Each View: Node Clustering and Similarity Search. The lower part is copied from Table 2.

Overall Performance

We evaluate the overall performance of the proposed methods at both multiplex graph level and single view level.

Multiplex Graph Level. The overall performance for all the comparison methods is presented in Table 2, where the upper and middle parts are comprised of the methods for graphs and multiplex graphs respectively. DGI and HDI are the building blocks of DMGI/DMGI$_{attn}$ and HDMI. DMGI/DMGI$_{attn}$ and HDMI perform better than DGI and HDI in general, demonstrating the effectiveness of joint modeling of different views.

Graph-PCL independently models each view and then combines embeddings from different views. It outperforms the baseline methods on ACM, IMDB, and Amazon, and it is slightly better than the second-best multiplex graph method, i.e., DMGI$_{attn}$, on DBLP. Graph-MVP$_{hard}$ and Graph-MVP$_{soft}$ jointly model different views, but they employ different semantic constraints. They perform similarly on IMDB and Amazon, while Graph-MVP$_{hard}$ is better on DBLP and Graph-MVP$_{soft}$ is better on ACM. These results demonstrate the effectiveness of the proposed PCL and semantic constraints for modeling multiplex graphs.

Table 5: Ablation Study on the PAP view of ACM

	MaF1	MiF1	NMI	S@5
Graph-PCL	0.908	0.908	0.735	0.917
w/o warm-up	0.863	0.865	0.721	0.903
w/o $\mathcal{L}_{\mathcal{S}}$	0.865	0.867	0.693	0.899
w/o $\mathcal{L}_{\mathcal{N}}$	0.878	0.880	0.678	0.881
1st-order GCN (ReLU)	0.865	0.866	0.559	0.859
GCN (Tanh)	0.881	0.881	0.486	0.886
GCN (ReLU)	0.831	0.831	0.410	0.837
masking	0.888	0.890	0.716	0.903
w/o attribute drop	0.843	0.845	0.568	0.869
w/o adj. matrix drop	0.888	0.888	0.715	0.903

(a) MaF1 v.s. K (b) NMI v.s. K

Figure 3: The number of K on PSP and PAP of ACM

View Level. The experimental results for the single views are presented in the upper parts of Table 3-4. We only compare Graph-PCL with DGI and HDI because they are the backbones of DMGI/DMGI$_{attn}$ and HDMI, which have the best overall performance on the multiplex graphs. As shown in Table 3-4, it is evident that Graph-PCL outperforms the baseline methods on all the views for all the tasks. Both DGI and HDI are Infomax-based CL methods, and the superior performance of Graph-PCL indicates that the proposed PCL strategy is better than the Infomax-based strategy.

Ablation Study

We conduct ablation studies at both the multiplex graph level and the single view level.

Multiplex Graph Level. Firstly, we compare the joint modeling and simple combination for different views. As shown in Table 2, Graph-MVP$_{hard}$ and Graph-MVP$_{soft}$ obtain higher scores than Graph-PCL in most of the cases, which demonstrates that joint modeling different views are a better practice than the simple combination of them.

Secondly, we compare the performance of using multiple views and a single view in Table 3-4. On the one hand, the simple combination of different views might not improve the informativeness of the embeddings, which is demonstrated by comparing the performance of Graph-PCL on the single views and multiplex graphs. On the other hand, the performance of Graph-MVP$_{hard}$/Graph-MVP$_{soft}$ on multiplex graphs is much better than Graph-PCL's performance on the single views, which further demonstrates the importance of the joint modeling strategy.

View Level. We study the influence of different configurations of Graph-PCL on the PAP view of ACM. The results are presented in Table 5. Firstly, all of the warm-up, $\mathcal{L}_{\mathcal{S}}$ and $\mathcal{L}_{\mathcal{N}}$ are critical. Secondly, for different variants of GCN, the 1st-order GCN always perform better than GCN, and Tanh is better than ReLU. We believe this is because the 1st-order GCN has a better capability than GCN for capturing the attributes, and Tanh provides a better normalization for the node embeddings. Finally, for the configurations of the graph transformation, masking performs worse than dropout, and dropout on both attributes and adjacency matrix is important. Different from masking, dropout re-scales the outputs by $\frac{1}{1-p_{drop}}$, which improves the performance.

Number of Clusters

Figure 3 presents the MaF1 and NMI scores on the PSP and PAP view of ACM w.r.t. the number of clusters $K \in [3, 4, 5, 10, 30, 50]$. For PSP and PAP views of ACM, the best MaF1 and NMI scores are obtained when $K = 30$ and $K = 5$, respectively. The number of ground-truth classes for ACM is 3, and the results in Figure 3 indicate that over-clustering is beneficial. We believe this is because there are many sub-clusters in the embedding space, which is consistent with the prior findings on image data (Li et al. 2020).

Visualization

The t-SNE (Maaten and Hinton 2008) visualizations of the embeddings for the PSP and PAP views of ACM are shown in Figure 4. $\mathcal{L}_{\mathcal{N}}$ means that the encoder is trained only with the node-level loss. For Graph-PCL, the numbers of clusters for PSP and PAP are 30 and 5 since they produce the best performance as shown in Figure 3. We can observe that the embeddings extracted by Graph-PCL are better separated. The visualizations for the combined embeddings are shown in Figure 5. Embeddings in Figure 5a and Figure 5b are the concatenation of the view-specific embeddings in Figure 4. Generally, Graph-MVP$_{soft}$ has the best performance.

Related Work

Contrastive Learning for Graphs The goal of CL is to pull similar nodes into close positions in the embedding space and push dis-similar nodes far apart. We only review the most relevant works, for a comprehensive review, please refer to (Liu et al. 2021; Wu et al. 2021).

DGI (Veličković et al. 2018), GMI (Peng et al. 2020) and HDI (Jing, Park, and Tong 2021) obtain negative samples by randomly shuffling the node attributes. MVGRL (Hassani and Khasahmadi 2020) transforms graphs via techniques such as graph diffusion (Klicpera, Weißenberger, and Günnemann 2019). GraphCL (You et al. 2020) uses various graph augmentations to obtain positive nodes. GCA (Zhu et al. 2021) masks nodes and edges via their importance.

For multiplex graphs, MNE (Zhang et al. 2018a), MVN2VEC (Shi et al. 2018) and GATNE (Cen et al. 2019) sample node pairs based on random walks. DMGI (Park et al. 2020) and HDMI (Jing, Park, and Tong 2021) use random attribute shuffling to sample negative nodes.
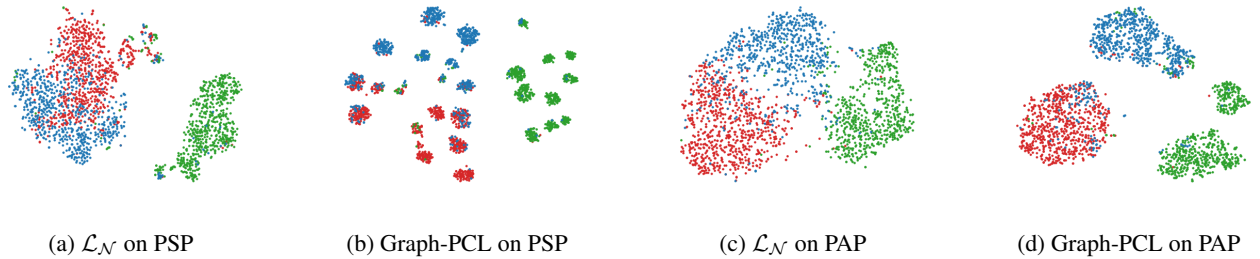
(a) $\mathcal{L}_{\mathcal{N}}$ on PSP   (b) Graph-PCL on PSP   (c) $\mathcal{L}_{\mathcal{N}}$ on PAP   (d) Graph-PCL on PAP

Figure 4: Visualization of the embeddings for PAP and PSP view of the ACM graph

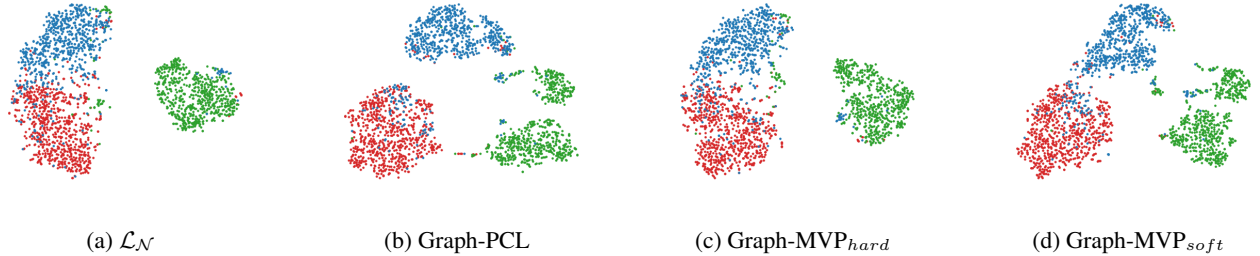(a) $\mathcal{L}_{\mathcal{N}}$ (b) Graph-PCL   (c) Graph-MVP$_{hard}$ (d) Graph-MVP$_{soft}$

Figure 5: Visualization of the combined embeddings for the ACM graph

Deep Clustering and Contrastive Learning. Clustering algorithms (Xie, Girshick, and Farhadi 2016; Caron et al. 2018; Wang et al. 2021), can capture the semantic clusters of instances. DeepCluster (Caron et al. 2018) is one of the earliest works which uses cluster assignments as "pseudo-labels" to update the parameters of the encoder. Inspired by these works, SwAV (Caron et al. 2020) and PCL (Li et al. 2020) combine deep clustering with CL. SwAV compares the cluster assignments rather than the embeddings of two images. PCL is the closest to our work, which alternatively performs clustering and parameter updating. However, PCL has some limitations: it is originally designed for single view image data; it heavily relies on data augmentations and momentum contrast (He et al. 2020); it has some complex assumptions over cluster distributions and embeddings.

Multiplex Graph Neural Networks. The multiplex graph considers multiple relations among nodes, and it is also known as the multi-view graph (Qu et al. 2017), multi-layer graph (Li et al. 2018), multi-dimension graph (Ma et al. 2018) and multiplex heterogeneous graph (Cen et al. 2019). MVE (Qu et al. 2017) and HAN (Wang et al. 2019b) uses attention mechanisms to combine embeddings from different views. mGCN (Ma et al. 2019) models both within and across view interactions. VANE (Fu et al. 2020) uses adversarial training to improve the comprehensiveness and robustness of the embeddings. Multiplex graph neural networks have been widely used in many applications (Du et al. 2021), such as graph alignment (Chu et al. 2019; Yan et al. 2021; Xiong, Yan, and Pan 2021), time series (Jing, Tong, and Zhu 2021), text summarization (Jing et al. 2021), abstract reasoning (Wang, Jamnik, and Lio 2020), global poverty (Khan and Blumenstock 2019) and bipartite graphs (Xue et al. 2021).

Deep Graph Clustering. Graph clustering aims at discovering communities or groups in graphs. SAE (Tian et al. 2014) and MGAE (Wang et al. 2017) first train a GNN, and then run a clustering algorithm over node embeddings to obtain the clusters. Graph clustering has also been used to improve the training for graph encoders. DAEGC (Wang et al. 2019a) and SDCN (Bo et al. 2020) jointly optimize clustering algorithms and the graph reconstruction loss. AGC (Zhang et al. 2019) adaptively finds the optimal order for GCN based on the intrinsic clustering scores. M3S (Sun, Lin, and Zhu 2020) uses clustering to enlarge the labeled data with pseudo labels. Both of the proposed Graph-PCL and Graph-MVP are also deep graph clustering methods. However, different from prior methods, Graph-PCL and Graph-MVP leverage clustering to improve contrastive learning. Additionally, prior works ignore the multiplexity of the graphs, which is considered by Graph-MVP.

Conclusion

We introduce a novel Multi-View Prototypical Contrastive Learning framework for multiplex graphs (Graph-MVP). We first present a Graph Prototypical Contrastive Learning (Graph-PCL) framework for each view of the multiplex graphs. Graph-PCL captures both node-level and semantic-level information, which is an EM algorithm alternatively performing clustering and encoder parameter updating. Graph-MVP is based on Graph-PCL, which jointly models different views of multiplex graphs with the insight that the view-specific embeddings of a given node should be semantically similar. The experimental results on real-world multiplex graphs demonstrate the effectiveness of the proposed methods.

References

Bo, D.; Wang, X.; Shi, C.; Zhu, M.; Lu, E.; and Cui, P. 2020. Structural deep clustering network. In *Proceedings of The Web Conference 2020*, 1400–1410.

Caron, M.; Bojanowski, P.; Joulin, A.; and Douze, M. 2018. Deep clustering for unsupervised learning of visual features. In *Proceedings of the European Conference on Computer Vision (ECCV)*, 132–149.

Caron, M.; Misra, I.; Mairal, J.; Goyal, P.; Bojanowski, P.; and Joulin, A. 2020. Unsupervised learning of visual features by contrasting cluster assignments. *arXiv preprint arXiv:2006.09882*.

Cen, Y.; Zou, X.; Zhang, J.; Yang, H.; Zhou, J.; and Tang, J. 2019. Representation learning for attributed multiplex heterogeneous network. In *Proceedings of the 25th ACM SIGKDD International Conference on Knowledge Discovery & Data Mining*, 1358–1368.

Chu, X.; Fan, X.; Yao, D.; Zhu, Z.; Huang, J.; and Bi, J. 2019. Cross-network embedding for multi-network alignment. In *The World Wide Web Conference*, 273–284.

De Domenico, M.; Solé-Ribalta, A.; Cozzo, E.; Kivelä, M.; Moreno, Y.; Porter, M. A.; Gómez, S.; and Arenas, A. 2013. Mathematical formulation of multilayer networks. *Physical Review X*, 3(4): 041022.

Dempster, A. P.; Laird, N. M.; and Rubin, D. B. 1977. Maximum likelihood from incomplete data via the EM algorithm. *Journal of the Royal Statistical Society: Series B (Methodological)*, 39(1): 1–22.

Du, B.; Zhang, S.; Yan, Y.; and Tong, H. 2021. New Frontiers of Multi-Network Mining: Recent Developments and Future Trend. In *Proceedings of the 27th ACM SIGKDD Conference on Knowledge Discovery & Data Mining*, 4038–4039.

Fu, D.; Xu, Z.; Li, B.; Tong, H.; and He, J. 2020. A View-Adversarial Framework for Multi-View Network Embedding. In *Proceedings of the 29th ACM International Conference on Information & Knowledge Management*, 2025–2028.

Grover, A.; and Leskovec, J. 2016. node2vec: Scalable feature learning for networks. In *Proceedings of the 22nd ACM SIGKDD*, 855–864.

Hamilton, W. L.; Ying, R.; and Leskovec, J. 2017. Representation learning on graphs: Methods and applications. *arXiv preprint arXiv:1709.05584*.

Hassani, K.; and Khasahmadi, A. H. 2020. Contrastive Multi-View Representation Learning on Graphs. *arXiv preprint arXiv:2006.05582*.

He, K.; Fan, H.; Wu, Y.; Xie, S.; and Girshick, R. 2020. Momentum contrast for unsupervised visual representation learning. In *Proceedings of the IEEE/CVF Conference on Computer Vision and Pattern Recognition*, 9729–9738.

Hu, W.; Liu, B.; Gomes, J.; Zitnik, M.; Liang, P.; Pande, V.; and Leskovec, J. 2019. Strategies for pre-training graph neural networks. *arXiv preprint arXiv:1905.12265*.

Jiao, Y.; Xiong, Y.; Zhang, J.; Zhang, Y.; Zhang, T.; and Zhu, Y. 2020. Sub-Graph Contrast for Scalable Self-Supervised Graph Representation Learning. In *2020 IEEE International Conference on Data Mining (ICDM)*, 222–231.

Jing, B.; Park, C.; and Tong, H. 2021. Hdmi: High-order deep multiplex infomax. In *Proceedings of the Web Conference 2021*, 2414–2424.

Jing, B.; Tong, H.; and Zhu, Y. 2021. Network of Tensor Time Series. In *The World Wide Web Conference*.

Jing, B.; You, Z.; Yang, T.; Fan, W.; and Tong, H. 2021. Multiplex Graph Neural Network for Extractive Text Summarization. *arXiv preprint arXiv:2108.12870*.

Khan, M. R.; and Blumenstock, J. E. 2019. Multi-gcn: Graph convolutional networks for multi-view networks, with applications to global poverty. In *Proceedings of the AAAI Conference on Artificial Intelligence*, volume 33, 606–613.

Kipf, T. N.; and Welling, M. 2016. Semi-supervised classification with graph convolutional networks. *arXiv preprint arXiv:1609.02907*.

Klicpera, J.; Weißenberger, S.; and Günnemann, S. 2019. Diffusion improves graph learning. *Advances in Neural Information Processing Systems*, 32: 13354–13366.

Li, J.; Chen, C.; Tong, H.; and Liu, H. 2018. Multi-layered network embedding. In *Proceedings of the 2018 SIAM International Conference on Data Mining*, 684–692. SIAM.

Li, J.; Zhou, P.; Xiong, C.; and Hoi, S. C. 2020. Prototypical contrastive learning of unsupervised representations. *arXiv preprint arXiv:2005.04966*.

Liu, Y.; Pan, S.; Jin, M.; Zhou, C.; Xia, F.; and Yu, P. S. 2021. Graph self-supervised learning: A survey. *arXiv preprint arXiv:2103.00111*.

Ma, Y.; Ren, Z.; Jiang, Z.; Tang, J.; and Yin, D. 2018. Multi-dimensional network embedding with hierarchical structure. In *Proceedings of the eleventh ACM WSDM*, 387–395.

Ma, Y.; Wang, S.; Aggarwal, C. C.; Yin, D.; and Tang, J. 2019. Multi-dimensional graph convolutional networks. In *Proceedings of the 2019 SIAM International Conference on Data Mining*, 657–665. SIAM.

Maaten, L. v. d.; and Hinton, G. 2008. Visualizing data using t-SNE. *Journal of machine learning research*, 9(Nov): 2579–2605.

Meng, Z.; Liang, S.; Bao, H.; and Zhang, X. 2019. Co-embedding attributed networks. In *Proceedings of the Twelfth ACM International Conference on Web Search and Data Mining*, 393–401.

Park, C.; Han, J.; and Yu, H. 2020. Deep multiplex graph infomax: Attentive multiplex network embedding using global information. *Knowledge-Based Systems*, 197: 105861.

Park, C.; Kim, D.; Han, J.; and Yu, H. 2020. Unsupervised Attributed Multiplex Network Embedding. In *AAAI*, 5371–5378.

Paszke, A.; Gross, S.; Massa, F.; Lerer, A.; Bradbury, J.; Chanan, G.; Killeen, T.; Lin, Z.; Gimelshein, N.; Antiga, L.; et al. 2019. Pytorch: An imperative style, high-performance

deep learning library. *Advances in neural information processing systems*, 32: 8026–8037.

Peng, Z.; Huang, W.; Luo, M.; Zheng, Q.; Rong, Y.; Xu, T.; and Huang, J. 2020. Graph Representation Learning via Graphical Mutual Information Maximization. In *Proceedings of The Web Conference 2020*, 259–270.

Perozzi, B.; Al-Rfou, R.; and Skiena, S. 2014. Deepwalk: Online learning of social representations. In *Proceedings of the 20th ACM SIGKDD*, 701–710.

Qiu, J.; Chen, Q.; Dong, Y.; Zhang, J.; Yang, H.; Ding, M.; Wang, K.; and Tang, J. 2020. Gcc: Graph contrastive coding for graph neural network pre-training. In *Proceedings of the 26th ACM SIGKDD International Conference on Knowledge Discovery & Data Mining*, 1150–1160.

Qu, M.; Tang, J.; Shang, J.; Ren, X.; Zhang, M.; and Han, J. 2017. An attention-based collaboration framework for multi-view network representation learning. In *Proceedings of the 2017 ACM CIKM*, 1767–1776.

Shi, Y.; Han, F.; He, X.; He, X.; Yang, C.; Luo, J.; and Han, J. 2018. mvn2vec: Preservation and collaboration in multi-view network embedding. *arXiv preprint arXiv:1801.06597*.

Srivastava, N.; Hinton, G.; Krizhevsky, A.; Sutskever, I.; and Salakhutdinov, R. 2014. Dropout: a simple way to prevent neural networks from overfitting. *The journal of machine learning research*, 15(1): 1929–1958.

Sun, K.; Lin, Z.; and Zhu, Z. 2020. Multi-stage self-supervised learning for graph convolutional networks on graphs with few labeled nodes. In *Proceedings of the AAAI Conference on Artificial Intelligence*, volume 34, 5892–5899.

Tian, F.; Gao, B.; Cui, Q.; Chen, E.; and Liu, T.-Y. 2014. Learning deep representations for graph clustering. In *Proceedings of the AAAI Conference on Artificial Intelligence*, volume 28.

Veličković, P.; Cucurull, G.; Casanova, A.; Romero, A.; Lio, P.; and Bengio, Y. 2017. Graph attention networks. *arXiv preprint arXiv:1710.10903*.

Veličković, P.; Fedus, W.; Hamilton, W. L.; Liò, P.; Bengio, Y.; and Hjelm, R. D. 2018. Deep graph infomax. *arXiv preprint arXiv:1809.10341*.

Wang, C.; Pan, S.; Hu, R.; Long, G.; Jiang, J.; and Zhang, C. 2019a. Attributed graph clustering: A deep attentional embedding approach. *arXiv preprint arXiv:1906.06532*.

Wang, C.; Pan, S.; Long, G.; Zhu, X.; and Jiang, J. 2017. Mgae: Marginalized graph autoencoder for graph clustering. In *Proceedings of the 2017 ACM on Conference on Information and Knowledge Management*, 889–898.

Wang, D.; Jamnik, M.; and Lio, P. 2020. Abstract Diagrammatic Reasoning with Multiplex Graph Networks. In *International Conference on Learning Representations*.

Wang, X.; Ji, H.; Shi, C.; Wang, B.; Ye, Y.; Cui, P.; and Yu, P. S. 2019b. Heterogeneous graph attention network. In *The World Wide Web Conference*, 2022–2032.

Wang, Z.; Ni, Y.; Jing, B.; Wang, D.; Zhang, H.; and Xing, E. 2021. DNB: A Joint Learning Framework for Deep Bayesian Nonparametric Clustering. *IEEE Transactions on Neural Networks and Learning Systems*.

Wu, L.; Lin, H.; Gao, Z.; Tan, C.; Li, S.; et al. 2021. Self-supervised on Graphs: Contrastive, Generative, or Predictive. *arXiv preprint arXiv:2105.07342*.

Xie, J.; Girshick, R.; and Farhadi, A. 2016. Unsupervised deep embedding for clustering analysis. In *International conference on machine learning*, 478–487. PMLR.

Xiong, H.; Yan, J.; and Pan, L. 2021. Contrastive Multi-View Multiplex Network Embedding with Applications to Robust Network Alignment. In *Proceedings of the 27th ACM SIGKDD Conference on Knowledge Discovery & Data Mining*, 1913–1923.

Xue, H.; Yang, L.; Rajan, V.; Jiang, W.; Wei, Y.; and Lin, Y. 2021. Multiplex Bipartite Network Embedding using Dual Hypergraph Convolutional Networks. In *Proceedings of the Web Conference 2021*, 1649–1660.

Yan, Y.; Liu, L.; Ban, Y.; Jing, B.; and Tong, H. 2021. Dynamic Knowledge Alignment. In *AAAI*.

You, Y.; Chen, T.; Sui, Y.; Chen, T.; Wang, Z.; and Shen, Y. 2020. Graph contrastive learning with augmentations. *Advances in Neural Information Processing Systems*, 33: 5812–5823.

Zhang, H.; Qiu, L.; Yi, L.; and Song, Y. 2018a. Scalable Multiplex Network Embedding. In *IJCAI*, volume 18, 3082–3088.

Zhang, X.; Liu, H.; Li, Q.; and Wu, X.-M. 2019. Attributed graph clustering via adaptive graph convolution. *arXiv preprint arXiv:1906.01210*.

Zhang, Z.; Yang, H.; Bu, J.; Zhou, S.; Yu, P.; Zhang, J.; Ester, M.; and Wang, C. 2018b. ANRL: Attributed Network Representation Learning via Deep Neural Networks. In *IJCAI*, volume 18, 3155–3161.

Zhu, Y.; Xu, Y.; Yu, F.; Liu, Q.; Wu, S.; and Wang, L. 2021. Graph contrastive learning with adaptive augmentation. In *Proceedings of the Web Conference 2021*, 2069–2080.

Zhuang, C.; and Ma, Q. 2018. Dual graph convolutional networks for graph-based semi-supervised classification. In *Proceedings of the 2018 World Wide Web Conference*, 499–508.